Available online at www.sciencedirect.com

ScienceDirect

Geochimica et Cosmochimica Acta 309 (2021) 299–312

Geochimica et Cosmochimica Acta

www.elsevier.com/locate/gca

The Mg/Ca proxy for temperature: A *Uvigerina* core-top study in the Southwest Pacific

Cassandre R. Stirpe [a], Katherine A. Allen [a], Elisabeth L. Sikes [b], Xiaoli Zhou [b,c], Yair Rosenthal [b], Alicia M. Cruz-Uribe [a], Hanna L. Brooks [a]

[a] *School of Earth and Climate Sciences, University of Maine, United States*
[b] *Department of Marine and Coastal Sciences, Rutgers University, United States*
[c] *School of Ocean and Earth Science, Tongji University, Shanghai, China*

Received 4 December 2020; accepted in revised form 9 June 2021; Available online 17 June 2021

Abstract

The Mg/Ca ratio of the infaunal benthic foraminifer *Uvigerina peregrina* is a commonly used proxy for reconstructing bottom water paleotemperatures because it is hypothesized to be insensitive to changes in bottom water carbonate chemistry. This study presents core-top *U. peregrina* samples from the southwest Pacific from 0.6 to 4.4 km water depth, corresponding to water temperatures of 1–9 °C. Samples from New Zealand's Bay of Plenty and Chatham Rise were compared to previous calibrations to assess Mg/Ca temperature sensitivity. Published core-top temperature sensitivities can explain *U. peregrina* Mg/Ca at a majority of our study sites, with the exception of sites at intermediate depths of ~2.4–3.3 km, where the Mg/Ca ratios are substantially higher than expected from these calibrations, possibly reflecting diagenetic or non-thermal effects. Stable isotope measurements ($\delta^{18}O$ and $\delta^{13}C$), laser ablation analyses, and scanning electron microscope imagery complement trace element measurements to assess variables potentially affecting *U. peregrina* Mg/Ca at these sites. Morphotype variability, contamination, dissolution, and recrystallization all failed to provide satisfactory explanations for anomalously high Mg/Ca observations. We infer that a non-temperature control, perhaps related to carbonate chemistry, may be affecting the Mg incorporation in some *U. peregrina* specimens, though no factor has yet been clearly identified. It is unclear whether the factor affecting these sites is constant through time or could vary. For this reason, we recommend that Mg/Ca of recent specimens at each core site should be checked against established calibration curves prior to pursuing down-core paleotemperature reconstructions using *U. peregrina*. Where possible, paleotemperature estimates should also be validated using other independent proxies. Existing core-top calibrations effectively predict *U. peregrina* Mg/Ca at the majority of our study sites, but our findings underscore the need for a more thorough understanding of non-temperature factors that can influence Mg/Ca in *U. peregrina*.

Keywords: Paleotemperature proxy; Paleoceanography; Foraminifera; Paleoclimate; Mg/Ca; Uvigerina peregrina

1. INTRODUCTION

Ocean temperature is a key parameter in Earth's ocean-climate system, past and present. A widely used tool for estimating past deep ocean temperatures is the magnesium to calcium ratio (Mg/Ca) of calcite produced by benthic foraminifera, including species within the genus *Uvigerina* (Lear et al., 2002; Elderfield et al., 2006; Bryan and Marchitto, 2008). When combined with the oxygen isotope composition of foraminiferal calcite ($\delta^{18}O_c$), Mg/Ca-based temperature reconstructions also enable estimation of the past isotopic composition of seawater ($\delta^{18}O_{sw}$), which is linked to global ice volume (*e.g.*, Elderfield et al., 2010; Elderfield et al., 2012). Such work is founded on

https://doi.org/10.1016/j.gca.2021.06.015
0016-7037/

calibrations that quantify the relationship between Mg/Ca in *Uvigerina* calcite and its growth environment (Rosenthal et al., 1997a; 1997b; Lear et al., 2002; Elderfield et al., 2006; Bryan and Marchitto, 2008).

Refining calibrations for deep water masses is important to the field of paleoceanography because discerning temperature changes in the deep ocean requires a precise proxy. Bottom water temperatures today are cold, and only small (~2 °C) differences in temperature are expected between recent glacial and interglacial periods (Shackleton, 1987; Waelbroeck et al., 2002), requiring a precise proxy to detect them. Different Mg/Ca-temperature sensitivities have been observed in populations of *Uvigerina* spp. inhabiting different ocean regions (Fig. 1; Table S1), suggesting that region-specific calibrations are necessary due to cryptic species differences and/or that apparent differences in sensitivity are caused by an unidentified, non-temperature variable. The *Uvigerina peregrina* species encompasses a variety of morphotypes (Schweizer et al., 2005; Williams et al., 1988), and it has been hypothesized that these morphotypes may also be characterized by differences in Mg incorporation (Elderfield et al., 2012). In this study, we build on prior calibration efforts with *Uvigerina* (Lear et al., 2002; Elderfield et al., 2006; Bryan and Marchitto, 2008; Elderfield et al., 2010; Gussone et al., 2016) with the aim to refine the proxy with new core-top Mg/Ca measurements from the southwest Pacific.

Uvigerina peregrina is infaunal, typically living within the upper centimeters of sediment (*e.g.,* McCorkle et al., 1990). Its infaunal habitat means that it is immersed in sediment pore waters rather than being bathed by bottom waters. However, the diffusion of seawater into sediments establishes a link between *U. peregrina* specimens and the overlying water mass. Elderfield et al. (2006) suggested that *Uvigerina*'s carbonate-buffered infaunal habit makes it a particularly good archive for temperature signals because it can record physical properties of deep water masses while remaining protected from changes in deep-water carbonate saturation. It has been observed that $\Delta[CO_3^{2-}]$ ($\Delta[CO_3^{2-}] = [CO_3^{2-}]_{in\ situ} - [CO_3^{2-}]_{sat}$) of pore waters can be lower than $\Delta[CO_3^{2-}]$ of overlying bottom waters (Weldeab et al., 2016). In addition, the infaunal habitat of *Uvigerina* has the potential to expose it to different redox conditions than epifaunal foraminifer species, particularly in areas with high rates of organic matter deposition and remineralization (e.g., Jorissen et al., 1995; Koho et al., 2008). The influences on Mg/Ca in infaunal foraminifera may therefore be more complex and variable than previously assumed. However it should be noted that even if $\Delta[CO_3^{2-}]$ is variable, *Uvigerina* appears to be largely unaffected by this parameter (Elderfield et al., 2010).

Core-top calibrations using *Uvigerina* spp. have yielded Mg/Ca sensitivities ranging from 0.044 – 0.096 mmol/mol per ℃ (Bryan and Marchitto, 2008; Elderfield et al., 2006; Yu and Elderfield, 2008; Elderfield et al., 2010). Bryan and Marchitto (2008) suggested that sensitivity may not be uniform across the ocean's full temperature range, with some observations suggesting higher sensitivity at lower temperatures. A down-core calibration (Elderfield et al., 2010) determined a higher Mg/Ca sensitivity to temperature

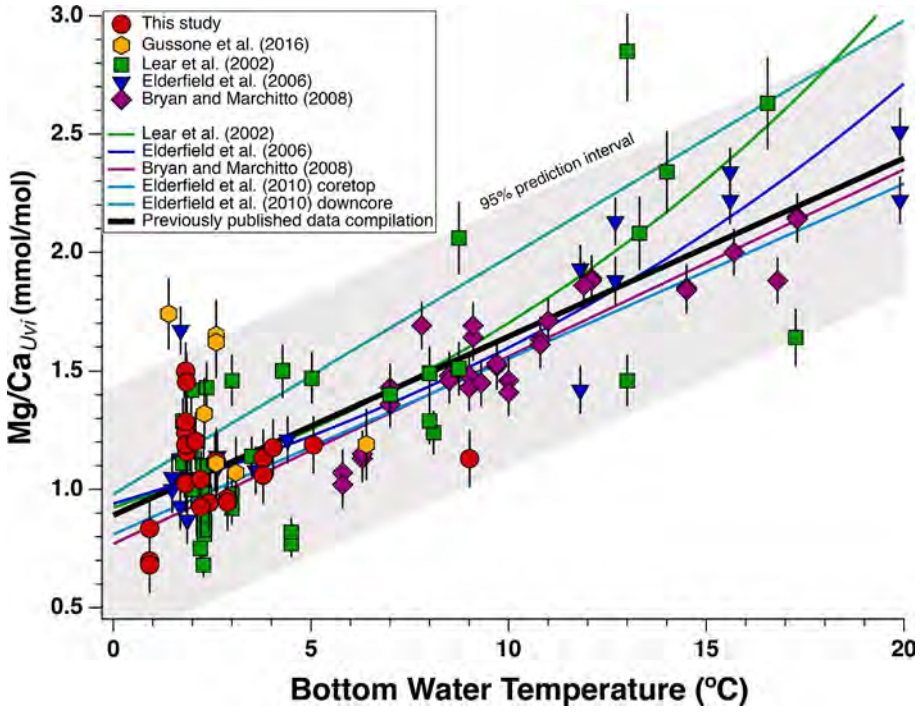

Fig. 1. Mg/Ca (mmol/mol) of coretop *Uvigerina* vs bottom water temperature (°C). Previously published data and calibration equations are included. A linear regression (black) was generated for all previously published data, and a 95% prediction interval was determined (gray shaded area). Mg/Ca data obtained in this study (red circles) are from New Zealand's Bay of Plenty and Chatham Rise, with ± 0.12 mmol/mol (2SD from replicates). All values and calibrations are from core-top measurements, unless otherwise noted.

(0.1 mmol/mol per °C) than that found using a core-top approach (0.074 ± 0.04 mmol/mol per °C). The higher sensitivity has been used to generate down-core temperature reconstructions from the southwest Pacific on the basis of two arguments: that modern calibrations contain few or no observations at the low temperatures likely characterizing the glacial ocean and that application of the 0.1 mmol/-mol per °C sensitivity yields results consistent with pore-water-based $\delta^{18}O_{sw}$ estimates (Elderfield et al., 2010; Elderfield et al., 2012). Such arguments are reasonable; however, the core-top vs. down-core discrepancy remains unexplained, as do differences among core-top studies. It is possible that an additional variable (such as $\Delta[CO_3^{2-}]$) is influencing apparent Mg/Ca sensitivity. The present core-top study seeks to explore apparent discrepancies in sensitivity and determine if published calibration equations are appropriate for *U. peregrina* located in the southwest Pacific.

Our *U. peregrina* calibration is based on a suite of sediment multi-cores stretching from the Bay of Plenty to the Chatham Rise (Fig. 2). Collectively, these cores span a depth range of 663 m to 4375 m, corresponding to a modern temperature range of ~ 9 °C to 1 °C. Most of the sites are in deep waters at temperatures < 4 °C. This range of site depths captures multiple water masses originating in both the Pacific and Southern Oceans. Core names, depths, and locations are listed in Table S2.

Although modern deep water masses show little temperature variation, they can be distinguished by their chemical properties (Fig. S1). The concentrations of dissolved oxygen and inorganic carbon can differentiate between the chemically-aged Pacific Deep Water (PDW) with elevated dissolved inorganic carbon (DIC) content and the more recently-ventilated, relatively low DIC water masses from the Southern Ocean, namely Antarctic Intermediate Water (AAIW) and Circumpolar Deep Water (CDW) (Talley, 2013). These core sites are ideally positioned for capturing changes in both northern-sourced and southern-sourced water masses, making it a valuable location for paleoceanographic reconstructions (*e.g.,* Allen et al., 2015; Sikes et al., 2016a; 2016b; Sikes et al., 2017; McCave et al., 2008; Skinner et al., 2014). *Uvigerina* are abundant in these cores and can provide data on the physical and chemical properties of water masses through time, complementing existing records.

In this study, we present core-top trace element data (including Mg/Ca) from multiple morphotypes of *U. peregrina*. Unexpectedly high Mg/Ca measurements at some sites prompted a more in-depth analysis of the samples. Specimens were studied for evidence of contamination or recrystallization, and multiple hypotheses were tested. In addition, tests of the planktonic foraminifer *Globorotalia inflata* from the same samples were analyzed to determine whether high-Mg secondary overgrowths could account for the higher-than-expected Mg/Ca ratios in the *U. peregrina*. While it is difficult to positively identify the cause of the high Mg/Ca ratios in *U. peregrina* at some of our core sites, we take steps to rule out several possibilities

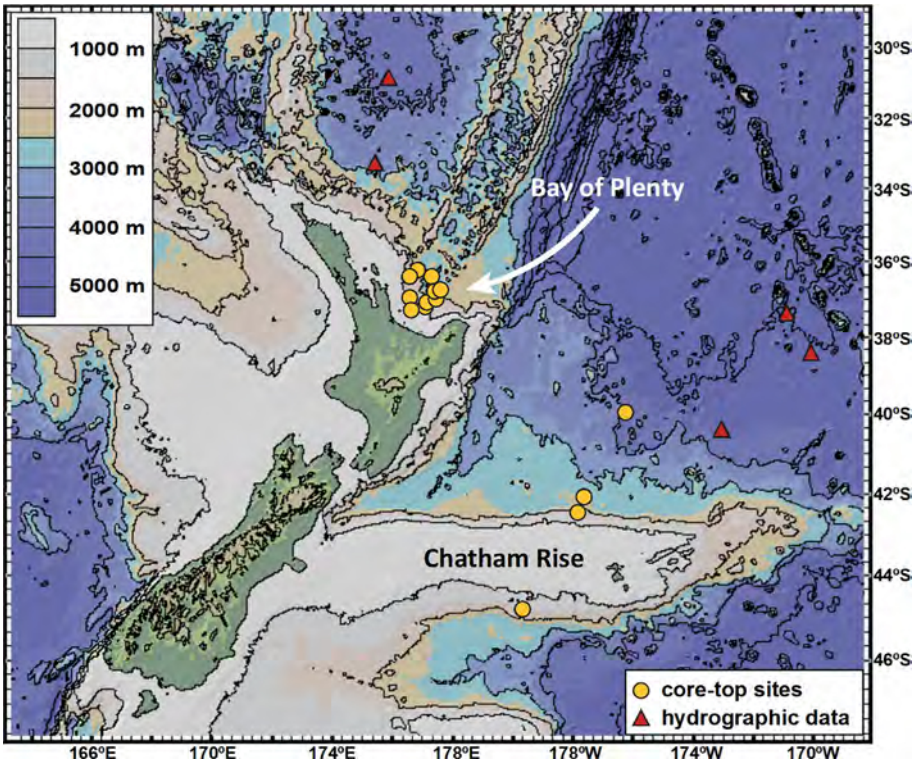

Fig. 2. Locations of New Zealand core-top sites. Sites include locations in the Bay of Plenty and across Chatham Rise, ranging in water depth from 663 m to 4375 m. Contour lines are drawn at 1000 m depth intervals. Also shown are sites used for hydrographic data. Figure created using GeoMapApp (www.geomapapp.org) and GMRT bathymetry (Ryan et al., 2009).

through the use of multiple analytical techniques. We conclude with recommendations regarding the future use of *U. peregrina* Mg/Ca in paleotemperature reconstructions.

2. METHODS

2.1. Stable isotope analysis

Sediments were washed with deionized water through a 63 μm sieve, and single species foraminiferal specimens were selected from the >250 μm fraction under a light microscope. A total of 27 samples of 1 to 3 specimens of *U. peregrina* were run for the 15 core-top sites. Samples were rinsed with distilled water and briefly sonicated (~3 pulses of 1 second each), to remove foreign material without damaging the specimens, and samples dried overnight at 35 °C prior to analysis. Carbon and oxygen stable isotopes were analyzed at the Rutgers University Stable Isotope Laboratory on a Micromass Optima Mass Spectrometer equipped with an automated Multiprep system. Results are presented in standard δ notation, relative to the Vienna PeeDee Belemnite (VPDB) standard, compared to an internal lab standard calibrated with NBS-19. The internal lab standard is offset from NBS-19 by 0.1 ‰ for $\delta^{13}C$ and 0.04 ‰ for $\delta^{18}O$. The 1-sigma precision of standards is typically 0.05 ‰ for $\delta^{13}C$ and 0.09 ‰ for $\delta^{18}O$.

2.2. Trace element analysis

Specimens were selected from the >250 μm size fraction. The *U. peregrina* samples comprised 8–10 individuals. *Globorotalia inflata* samples comprised ~150 individuals (weighing ~2–3 mg). In total, there were 25 *U. peregrina* and 9 *G. inflata* samples from 15 and 6 core-top sites, respectively.

Specimens were gently crushed between two glass slides prior to cleaning to break open the foraminifer tests and enable thorough cleaning of chamber interiors. Samples were cleaned following the methods of Boyle and Keigwin (1985) and Rosenthal et al. (1997a; 1997b) in a procedure using rinses with ultrapure water and methanol, followed by reductive and oxidative cleaning steps (see Supplementary Material Section 1 for details). Samples were analyzed using a Thermo Scientific Element XR ICP-MS located at Rutgers University.

Standard gravimetrically prepared solutions (4 mM Ca, Mg/Ca = 6.03 mmol/mol) were analyzed every five samples and were used to convert counts-per-second (cps) ratios into molar ratios following Rosenthal et al., (1999). No blank corrections were made. The average intensity of ^{25}Mg was ~ 5000 ± 200 (2 SE) cps for blanks and ~ 890,000 ± 77,000 (2 SE) cps for samples. Multiple matrix standards were run to account for any effects due to differing concentrations of calcium (Ca) in sample solutions. The average matrix correction for Mg/Ca was 6 %. Consistency standards with Mg/Ca of 1.44, 3.49, and 8.71 mmol/mol were analyzed at the beginning and end of each run. The two sets of consistency standards (from the beginning and end of the sample run, n = 2) were compared, yielding RSDs of 0.2, 1.2, and 0.9 %, respectively. Replicate samples of different specimens taken from the same cores show differences in Mg/Ca ranging from 0.02 to 0.11 mmol/mol (Table S6), with an average standard deviation of 0.06 mmol/mol. This is greater than the long-term analytical uncertainty of ~ 0.01–0.02 mmol/mol (~1–2 %).

2.3. Morphology

It has been observed that hispid *Uvigerina* spp. morphotypes may incorporate less Mg relative to costate and hispidocostate forms (Elderfield et al., 2012). We evaluated the role of morphotype differences on variability in the Mg/Ca ratios in the species by analyzing three separate *U. peregrina* morphotypes, designated Type A, Type B, and Type C (Fig. S2). Type A was the most common, occurring in every core, and defined as being primarily costate, but hispid on the terminal 1–3 chambers. Type B was more common in deeper cores, and was defined as being primarily hispid, with costae only poorly defined. Type C was more common in shallow cores, and was defined as being solely costate, and somewhat wider and shorter than the other morphotypes. The morphotypes were run separately in both trace element and stable isotope studies so their compositions could be compared.

2.4. SEM imaging and EDS compositional analysis

A Cameca SX-100 scanning electron microscope (SEM) at the University of Maine's School of Earth and Climate Sciences was used for imaging foraminifer specimens for signs of diagenetic alteration (*e.g.,* dissolution, overgrowths, etc.) and assessing the effectiveness of the trace element cleaning process. The Energy Dispersive X-Ray Spectroscopy (EDS) detector was used to identify compositional elements within suspected contaminants and categorize them by general composition.

Following an initial visual observation and designation, *U. peregrina* specimens from six cores were selected, lightly crushed, and then divided into two groups for partial cleaning and full cleaning. The partial cleaning consisted of rinsing and sonication, to remove foreign carbonates and aluminosilicate contaminants. The full cleaning followed the procedure described above in section 2.2, except for the final dissolution. Cleaned specimens were mounted to a glass slide for SEM imaging and comparison of cleaning techniques and their effectiveness at removal of visible contaminants.

2.5. Laser ablation ICP-MS

Fifteen *U. peregrina* specimens from three core-top sites were chosen from wet-sieved samples for laser ablation, without additional cleaning. Samples were ablated at the University of Maine MAGIC (MicroAnalytical Geochemistry and Isotope Characterization) Lab using an ESI NWR 193^{UC} system coupled to an Agilent 8900 ICP-MS/MS. The instrumental operation conditions are summarized in Table S3 (Supplementary Material).

Foraminifer chamber walls exposed in cross-section were targeted, and care was taken to avoid contact with the inner or outer test surfaces, which might be coated with contaminants (Fig. S3). The intention was to obtain scans of pure interior foraminiferal calcite, to be compared with results using solution methods in which an entire test is dissolved. Lines were ablated using an 8 μm round beam within chamber walls at a rate of 2–3 μm/s. The composition of each line was averaged and considered as a single "spot". Additional details are available in the Supplementary Material.

2.6. Hydrographic data

Hydrographic data were retrieved and visualized in Ocean Data View 5 (Schlitzer, 2018) using data from GLODAP v2.2019 (Olsen et al., 2019). The nearest station with the required data at the appropriate depth range was chosen from GLODAP to correspond with the core sites of this study and previous Mg/Ca calibrations (Lear et al., 2002; Elderfield et al., 2006; Bryan and Marchitto, 2008). On average, the hydrographic profiles were located ~400–450 km from the core-top locations. Carbonate system parameters were calculated using the nearest appropriate GLODAP site measurements of alkalinity, DIC, pH, temperature, and pressure, using the constants of Dickson et al. (2007). Oxygen isotope data were retrieved from NASA's Global Seawater Oxygen-18 database (Schmidt et al., 1999). All stations used are listed in Table S4. Linear interpolation between sampling depths created continuous profiles used to assign values to core-top depths. Cross sections running east–west and north–south were examined to assess whether water masses were laterally continuous between the hydrographic profiles and the core-top locations (Fig. S1).

2.7. Site selection and age control

The sites chosen are located in the waters off of New Zealand and are useful for a calibration study for multiple reasons. New Zealand volcanism provides an additional dating method for the cores (see below). The Bay of Plenty and Chatham Rise also offer the opportunity of obtaining cores at a variety of depths, making it possible to capture both intermediate and deep water masses. This is particularly important for this calibration study because it allowed us to capture a wide range of temperatures (9–1 °C). Finally, confirming a calibration equation for the southwest Pacific would facilitate paleoceanographic studies in this area.

Age constraints can be placed on the multi-core samples studied using complementary New Zealand piston cores and calculated sedimentation rates. The multi-cores studied have coordinating longer piston cores, for which many have both ^{14}C and tephrochronology available (Shane et al., 2006; Sikes et al., 2016a; 2016b). The following multicores (MCs) must be Holocene in age based on published, paired piston core (PC) chronologies: RR0503 86 MC/87 JPC (663 m), 78 MC/79 JPC (1165 m), 65MC/67JPC (1887 m), 104MC/107JPC (2472 m), and 122MC/125JPC (2541 m) (Table S2). For example, core 87 JPC contains an ash layer at 95 cm depth dated to ~ 7.0 kyr BP (Lowe et al., 2013), yielding an average sedimentation rate of 13.6 cm/kyr. The first centimeter of sediment from multicore 86 is thus expected to contain material from at least the past ~75 years, certainly younger than 7.0 kyr. It should be noted that these are maximum ages, because piston coring often results in the disturbance and/or compaction of the uppermost, youngest sediments. It is expected that surface multicore sediments are younger than the uppermost piston core sediments.

The downcore dates from piston cores confirm that for these 5 multi-cores the material is Holocene in age. An additional four multi-cores have other tephra marker beds that can be used to help constrain their ages (Table S2). Based on average accumulation rates, and taking into account bioturbation and other mixing effects, it is expected that the core-top material from 0-1 cm depth should contain foraminifera from the past several hundred years. In addition, isotopic records in this region (e.g., Sikes et al., 2016a; 2016b) suggest that intermediate and deep water conditions have been stable since the mid-Holocene. Although age control is not available for the other multicore sites, *U. peregrina* $\delta^{18}O$ measurements are consistent with foraminifera that calcified under modern or near-modern conditions (Fig. 3, Table S5).

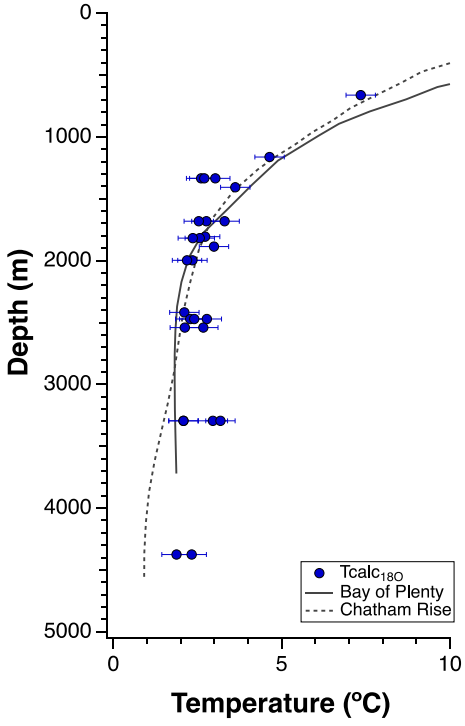

Fig. 3. Depth profiles showing temperature and $\delta^{18}O$-derived temperature ($Tcalc_{18O}$), calculated using Equation 1, from Marchitto et al. (2014). $\delta^{18}O$-derived temperature was calculated using $\delta^{18}O_{Uvi}$ and $\delta^{18}O_{sw}$.

3. RESULTS

3.1. Stable Isotopes ($\delta^{18}O$ and $\delta^{13}C$)

Between the shallowest site (663 m) and 2000 m, $\delta^{18}O_{Uvi}$ increases rapidly from 2.1 to 3.2 ‰ (Fig. S4, Table S5). Below 2000 m, values fall within a narrower range (3.0–3.3 ‰). Replicate samples of the same morphotype reproduced $\delta^{18}O_{Uvi}$ within ± 0.1 ‰, similar to the 1-σ analytical precision of 0.09 ‰. The largest differences between replicates were −0.25 ‰ and 0.18 ‰, between morphotypes A and B, and A and C, respectively.

The following equation derived from Marchitto et al. (2014) was used to derive temperature from measured $\delta^{18}O_{Uvi,}$ and modern $\delta^{18}O_{sw}$:

$$T = 16.28 + \frac{(\delta^{18}O_{SW} - \delta^{18}O_{Uvi})}{0.231} \quad (1)$$

$\delta^{18}O_{Uvi}$-based temperature estimates mimic the temperature profiles of nearby hydrographic stations. The reproduced water temperatures are within ±0.5 °C in 15 of 27 samples, and within ±1.0 °C in 21 of 27 samples from the *in situ* temperature profiles (Fig. 3). The largest difference between calculated and measured temperature was −1.66 °C, at a depth of 663 m (Fig. 3).

$\delta^{13}C_{Uvi}$ decreases with depth from a maximum of 0.67 ‰ at 663 m to a minimum of approximately −0.83‰ at 3295 m within the Bay of Plenty (Table S5). Below this depth, $\delta^{13}C_{Uvi}$ increases to a value of −0.26‰ at 4375 m on Chatham Rise (Fig. S5). The difference between replicates of the same morphotype averaged 0.14 ‰ (maximum 0.33 ‰) and replicates between morphotypes averaged 0.28 ‰ (maximum 0.42 ‰). The $\delta^{13}C_{Uvi}$ depth profile is similar to that of $\delta^{13}C_{sw}$ (Fig. S5), with a negative offset ranging from −0.45 to −1.26 ‰.

3.2. Trace elements: whole-shell analysis by solution ICP-MS

3.2.1. Uvigerina

Overall, Mg/Ca of *U. peregrina* ranges from 0.68 – 1.50 mmol/mol (Table S6). For 13 of 25 samples (60 %), measured Mg/Ca agrees with previously published calibration lines, within analytical error and calibration uncertainty (Fig. 4). A notable feature of the New Zealand Mg/Ca dataset is the anomalously high Mg/Ca between 2.4 and 3.3 km, with an average of ~ 1.26 mmol/mol and a maximum of 1.50 mmol/mol at bottom water temperatures of ~1.8 °C (Fig. S6). Similarly high Mg/Ca is found in other datasets, particularly in Lear et al. (2002), Elderfield et al. (2006), and Gussone et al. (2016) at the same temperature of ~2 °C (Fig. 1, Fig. S6). Our Mg/Ca values between 2.4 and 3.3 km exceed those expected for 2 °C conditions based on previously published calibration curves (Fig. 1; Fig. S6) similar to Mg/Ca measurements from other sites that also show elevated Mg/Ca at these temperatures.

The Mg/Ca measurements were screened for Mg-bearing contaminant phases using Al/Ca, Ti/Ca, Mn/Ca, and Fe/Ca (Table S6). These ratios showed no clear correlation with Mg/Ca ($R^2 < 0.2$ in all cases; Fig. S7). Potential contamination was identified using the outlier method of Tukey (1977) which uses quartiles and inter-quartile range to determine outliers. These outlier thresholds were 95.2, 3.6, 18.9, and 29.6 µmol/mol for Al/Ca, Ti/Ca, Mn/Ca, and Fe/Ca, respectively. Based on these values, 3 out of 25 samples were flagged with two contaminants above the thresholds, and an additional 7 samples were flagged with one contaminant above the thresholds. However, excluding samples on the basis of contaminant indicators does not change or remove the anomalously high Mg/Ca signal at ~2 °C (Fig. S8). For the purposes of this study, no samples were excluded from discussion because the variation of contaminant indicators cannot adequately explain the pattern of Mg/Ca distribution at the study sites.

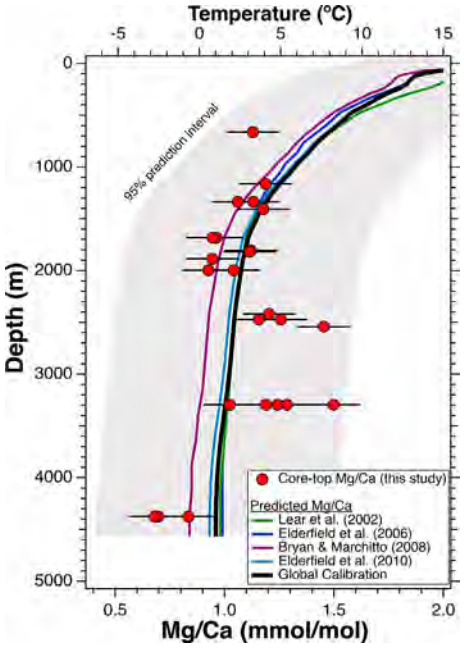

Fig. 4. Depth profile of Mg/Ca measured on *U. peregrina*. Also included are predicted Mg/Ca profiles, determined using previous core-top calibration equations (Lear et al., 2002; Elderfield et al., 2006; Bryan and Marchitto, 2008; Elderfield et al., 2010) and local temperature profiles. The 95% prediction interval is shaded in gray. The temperature axis is aligned to the global calibration equation. Error bars are 0.12 mmol/mol (2SD from replicates).

Our three broadly defined *U. peregrina* morphotypes (hispidocostate, hispid, and costate; as in Fig. S2) were analyzed separately to assess potential geochemical differences among them. No consistent offset is observed among the different morphotypes in either trace elements or stable isotopes (Fig. S9; Fig. S10). Lacking a consistent offset among morphotypes, data derived from all three groups are plotted and discussed as a single population throughout the remainder of the text.

3.2.2. Globorotalia inflata

G. inflata calcify at ~250–500 m (Anand et al., 2003; Cléroux et al., 2007; Groeneveld and Chiessi, 2011), which in this region corresponds to temperatures of approximately 11–16 °C (Olsen et al., 2019). The species-specific

equation from Groeneveld and Chiessi (2011) was used to estimate the expected Mg/Ca value of *G. inflata*:

$$Mg/Ca = 0.72e^{(0.076*T)} \quad (2)$$

Assuming an average calcification temperature of 13 °C yields an average expected Mg/Ca of 1.9 mmol/mol, with expected Mg/Ca for 11–16 °C ranging from 1.6–2.4 mmol/mol. The Mg/Ca of analyzed *G. inflata* ranged from 1.30 to 1.88 mmol/mol. The average Mg/Ca from all six sites was 1.68 ± 0.17 mmol/mol (±2 SE), which translates to a calcification temperature of ~ 11 °C (Table S7). Samples from 2418 m and 3295 m water depths yielded lower Mg/Ca than the other four sites, averaging 1.35 ± 0.11 mmol/mol (±2 SE) (Fig. S11), corresponding to 8.3 °C. For the four cores at water depths < 2000 m, Mg/Ca ratio averaged 1.84 ± 0.05 mmol/mol (±2 SE), corresponding to 12.3 °C.

3.3. Scanning electron microscopy and energy-dispersive X-Ray spectroscopy

SEM imaging of uncleaned specimens revealed that only the deepest *U. peregrina* sample (4375 m) showed noticeable dissolution (Fig. S12). Planktonic foraminifera exhibited partial dissolution beginning at a depth of ~2 km. Imaging of the interiors revealed coatings on the interior wall of some chambers (Fig. S12, Fig. S13). The SEM and attached Energy Dispersive X-Ray Spectroscopy (EDS) revealed that the coatings on *G. inflata* are different from those on *U. peregrina*, both structurally and compositionally.

Coatings on the interior of a *U. peregrina* specimen (Fig. S13) from 3295 m were consistent with an aluminosilicate (Fig. S13) containing minor amounts of Mg, K, and Na (1.3 ± 1.8 wt%, 0.93 ± 0.29 wt%, and 0.47 ± 0.28 wt % respectively) in addition to Si, Al, and Fe. The Mg/Ca ratio was 180 ± 75 mmol/mol. The interior coating of a *G. inflata* specimen (Fig. S13) from 2418 m indicated almost pure $CaCO_3$ (97–99 wt%), with only trace amounts of other cations (e.g. Na, Mg, K, Al, Fe, each < 1 wt%). EDS Mg content averaged 0.36 ± 0.22 wt%, yielding Mg/Ca of 14 ± 10 mmol/mol. This is higher than foraminiferal calcite, but consistent with inorganic calcite (Oomori et al., 1987). Further SEM/EDS analyses on partially cleaned and fully cleaned *U. peregrina* specimens revealed that fully cleaned specimens showed greater wear to the tests, with rounded edges and evidence of partial dissolution whereas specimens that had only been rinsed and sonicated (partial cleaning) appeared better-preserved (Fig. S14).

3.4. Laser-ablation ICP-MS

Laser ablation revealed that the distribution of Mg within *U. peregrina* calcite is not uniform (Fig. 5). Intra-specimen range averaged 0.54 ± 0.13 mmol/mol (±2 SE), with a maximum and minimum of 0.98 and 0.25 mmol/mol, respectively (Table S8). Most variability occurred between different chambers. Where multiple ablation lines were drawn on the same chamber, the average intra-chamber range of Mg/Ca is 0.19 mmol/mol ± 0.06 mmol/mol (±2 SE). Differences between chambers range from 0.3-0.9 mmol/mol, largely dependent on distance between the chambers, with neighboring chambers exhibiting a more similar composition. Analytical uncertainty for each ablation line averaged ±0.07 mmol/mol.

An initial approximation of the average test composition of an individual was obtained using the mean of all ablation lines on a single specimen. The results are summarized in Table 1. The average Mg/Ca for sites 78D (1163 m), 114F (3295 m), and 38C (4375 m) were 1.49 ± 0.29, 1.28 ± 0.28, and 0.81 ± 0.21 mmol/mol (±2 SE), respectively.

3.5. Temperature estimation

Several previously published calibration equations, both linear and exponential, were used to assess how well *U. peregrina* Mg/Ca or Mg/Li could reproduce bottom water temperatures at our study sites (Lear et al., 2002; Elderfield et al., 2006; Bryan and Marchitto, 2008; Elderfield et al., 2010).

4. DISCUSSION

4.1. Temperature Control

The utility of benthic foraminiferal Mg/Ca as a paleotemperature proxy relies upon our ability to accurately translate the Mg/Ca of foraminiferal calcite to the organism's calcification temperature. Previous calibrations (e.g., Rosenthal et al., 1997a, 1997b; Lear et al. 2002; Elderfield et al., 2006; Bryan and Marchitto 2008) have demonstrated correlations between bottom water temperature and Mg/Ca of *Uvigerina* calcite from different ocean regions. The present study adds a new dataset from the southwest Pacific, including several sites located in deep and cold water masses.

A linear regression through previously published data yields the following relationship: Mg/Ca = 0.075 (±0.011) *BWT + 0.89 (±0.10) (R^2 = 0.70), which is indistinguishable from the core-top equation reported in Elderfield et al. (2010): Mg/Ca = 0.074 (±0.004)*BWT + 0.81 (±0.05) (R^2 = 0.96). Prediction intervals (Fig. 1) represent the region within which a new observation of the same population (*Uvigerina* Mg/Ca) will fall at a 95 % confidence level given a single predictor value (BWT). This range is larger than that for fitting coefficients alone because it takes into account expected random error associated with making a new observation. All of our new data fall within the 95 % prediction interval for the linear fit to previously published data (Fig. 1), demonstrating that the Mg/Ca-BWT relationship in *Uvigerina* from the southwest Pacific may be effectively represented by a global calibration; in other words, these foraminifera are not behaving as a distinct regional population with respect to Mg incorporation (see Supplementary Material Section 4).

A linear regression through the Mg/Ca data from only this study yields a low slope (0.02 mmol/mmol per °C) and low R^2 value (R^2 = 0.03). The low slope is due to the combination of high Mg/Ca values at ~ 2 °C, and the low Mg/Ca value at ~ 9 °C (Fig. S15). For these reasons, this regression should not be used for paleotemperature recon-

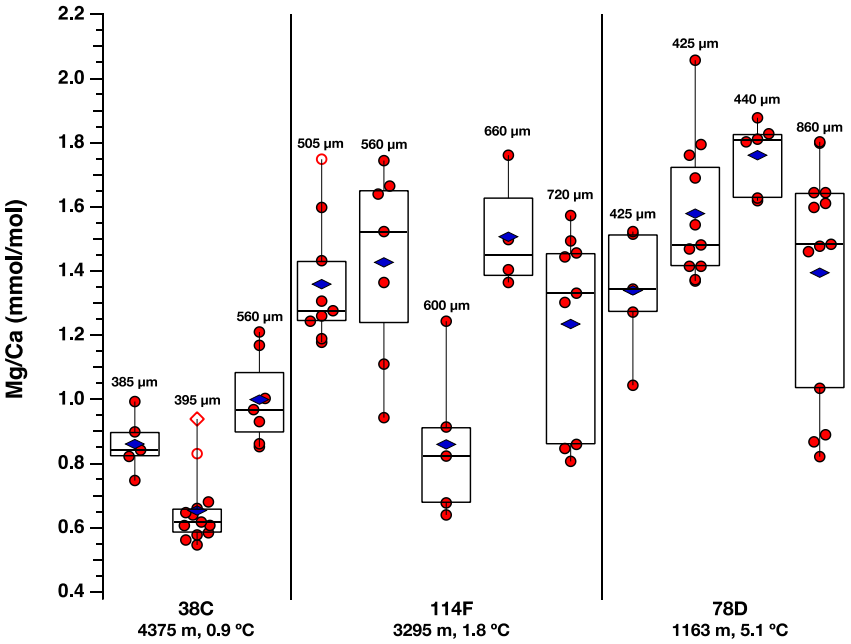

Fig. 5. Mg/Ca measured from *U. peregrina* laser ablation lines. Red markers indicate individual ablation line measurements. Each box represents a population of ablation lines from the same individual. Blue rhombuses indicate the mean Mg/Ca value for each individual *U. peregrina* specimen. Numbers above each box indicate the specimen's length. Black vertical lines separate specimens from different sites. Open symbols represent outliers and far outliers, defined using the interquartile range, as in Tukey (1977).

Table 1
Comparison of laser ablation (LA) ICP-MS and solution ICP-MS results. LA ICP-MS specimen averages are the mean Mg/Ca value across all ablation lines on a given individual *U. peregrina* test. Solution ICP-MS sample averages are the result of the dissolution of multiple individuals together. Site averages are the average of all measured Mg/Ca ratios for the site with the given method. In parentheses are given ± 2SE for each measurement and average.

Site, Depth	Laser Ablation ICP-MS		Solution ICP-MS	
	Specimen Averages	Site Average	Sample Averages	Site Average
78 D, 1163 m	1.34 (±0.18)	1.49 (±0.29)	1.19 (±0.02)	1.19 (±0.02)
	1.76 (±0.09)			
	1.39 (±0.20)			
	1.58 (±0.13)			
114F, 3295 m	1.51 (±0.18)	1.28 (±0.28)	1.24 (±0.02)	1.25 (±0.15)
	1.36 (±0.13)		1.50 (±0.03)	
	1.43 (±0.23)		1.19 (±0.02)	
	1.23 (±0.21)		1.28 (±0.03)	
	0.86 (±0.22)		1.02 (±0.02)	
38C, 4375 m	1.00 (±0.11)	0.81 (±0.22)	0.70 (±0.01)	0.74 (±0.10)
	0.86 (±0.08)		0.68 (±0.01)	
	0.66 (±0.06)		0.83 (±0.02)	

struction. However, the addition of the New Zealand data does not significantly affect the global calibration. If all data points are included in a linear regression, it yields the following equation: Mg/Ca = 0.073 (±0.037)*BWT + 0.90 (±0.04) (R^2 = 0.68). This further supports the conclusion that the New Zealand sites can be treated as part of a global dataset, despite the unexpectedly high Mg/Ca at the deeper sites.

Above a depth of 2000 m and temperature of ~2 °C, a global linear calibration may be applied to New Zealand core-top Mg/Ca to effectively predict BWT within ± 2 °C (Fig. 1; Fig. 4). The exception is a single sample from 663 m depth, which has low Mg/Ca resulting in a BWT estimate that is ~5 °C lower than observed. Calibration equations from Lear et al. (2002), Elderfield et al. (2006), Bryan and Marchitto (2008), and Elderfield et al. (2010) perform similarly well when comparing core-top *U. peregrina* Mg/Ca-based temperature estimates with modern temperature profiles from intermediate (1–2 km) New Zealand waters (see Supplementary Material Section 5). The Mg/Li-temperature equation of Bryan and Marchitto (2008) yielded an R^2 of 0.31, a lower T_{calc}:BWT ratio than

the Mg/Ca equations, and a higher y-intercept of 3.4 °C. All Mg/Li-calculated temperatures are overestimates at our sites, and offsets between measured and calculated temperatures are larger at greater depths (Fig. S16). For this *U. peregrina* dataset, Mg/Ca shows a stronger relationship to temperature ($R^2 = 0.44$) than Mg/Li ($R^2 = 0.31$). The highest R^2 for Mg/Ca predicted vs. observed temperatures is 0.44, implying that no matter which calibration is used (see Supplementary Material Section 5) a large proportion of the Mg/Ca variance in our New Zealand intermediate water (1–2 km) dataset is still not explained by temperature.

Below 2000 m, deviation of Mg/Ca-reconstructed temperature values from observed values is an average of 2.5 °C greater than it is for sites shallower than 2000 m. The sites between 2400 and 3300 m depth have Mg/Ca ratios higher than predicted from modern temperature profiles. Based on current calibrations and on Mg/Ca measurements from shallower New Zealand sites, temperature could only explain these high Mg/Ca values if the foraminifera originally calcified at temperatures greater than ~5 °C and depths shallower than ~1000 m, and then underwent transport to these deeper core sites. However, there is no evidence for downslope transport, with no sign of mechanical weathering or rounding. In addition, down-core records indicate no age reversals (Sikes et al., 2016a; 2016b). Significantly, isotope data are consistent with *in situ* formation (Fig. 3; Fig. S4; Fig. S5). We conclude that temperature alone cannot explain the high Mg/Ca ratios at the sites located between 2400 and 3300 m water depth.

Anomalously high-Mg *Uvigerina* samples are not unique to New Zealand (Fig. 1; Fig. S6). Similarly high Mg/Ca values were observed at ~2 °C in the northern Indian Ocean (Elderfield et al., 2006), the Sea of Okhotsk (Lear et al., 2002), and in the Cape Basin of the southeast Atlantic Ocean (Gussone et al., 2016). This persistent feature of *Uvigerina* Mg/Ca datasets, from multiple ocean basins, suggests that there is a non-temperature control that has yet to be identified.

4.2. Diagenetic effects

Diagenetic effects are unlikely to be the cause of the high Mg/Ca found at depth in this study. Partial dissolution, recrystallization, and contamination all fail to adequately explain the pattern observed.

Dissolution may explain lower-than-expected planktonic foraminifer Mg/Ca at these New Zealand sites, but there is little evidence that dissolution is exerting influence on *U. peregrina* Mg/Ca, except at the deepest site (4375 m). SEM analyses show no visual evidence of dissolution in *U. peregrina* above this depth. This is consistent with the comparison by Elderfield et al. (2006) of Rose-Bengal-stained (recently alive) and un-stained (older) core-top benthic foraminifera from high-carbonate-saturation and low-carbonate-saturation sites: there was no consistent Mg/Ca difference detected, indicating that *U. peregrina* is relatively resistant to dissolution and/or that Mg/Ca in shells of this species does not shift with dissolution. Dissolution is also unlikely to cause high Mg/Ca; prior studies have determined that partial dissolution preferentially decreases the Mg content of foraminiferal calcite (Berger, 1970; Brown and Elderfield, 1996; Johnstone et al., 2016; Regenberg et al., 2014; Sadekov et al., 2010). Calcite with a higher concentration of impurities is more soluble (e.g., Chave et al., 1962), and dissolves preferentially (Brown and Elderfield, 1996; Branson et al., 2015). Partial dissolution is therefore an unlikely explanation for the high Mg/Ca ratios seen in the core-top sites.

Recrystallization in marine sediments can occur at sites with simultaneous dissolution and reprecipitation. Recrystallization should increase Mg/Ca because inorganic calcite typically contains more Mg than foraminiferal calcite (Oomori et al., 1987). As foraminiferal calcite or other carbonate material dissolves, the components of calcite are released into sediment pore waters where they can reprecipitate as inorganic calcite. With a biogenic precursor, the new precipitate is likely to contain less Mg than if it had precipitated under other conditions (Raymo et al., 2018). However, it will still likely have a higher Mg/Ca value than the biologically formed foraminiferal calcite. The tests of the planktonic foraminifer *G. inflata* were deposited into the same sediment conditions, but they show no evidence of elevated Mg/Ca as would be expected in recrystallized specimens. Inorganic calcite was observed on a *G. inflata* specimen (Fig. S14), but the Mg/Ca values are not higher than predicted based on temperature control (Fig. S9). Crucially, at the depths where the *U. peregrina* show elevated Mg/Ca, *G. inflata* show lower Mg/Ca. This suggests that different processes are acting on the plankonic and benthic foraminifer specimens. No evidence of inorganic calcite precipitation such as blocky surface texture or crevice-filling was found on or inside *U. peregrina* tests under the SEM. It is possible for dissolution-reprecipitation reactions to occur without overt physical alteration (Chanda et al., 2019), but without conclusive evidence for recrystallization, we explore alternative answers to help explain the pattern of Mg/Ca observed.

Aluminosilicate contamination is another possible explanation for high Mg/Ca at the New Zealand sites, particularly given the quantity of ash present in the local sediments. Even with a rigorous cleaning procedure, it is not always possible to remove all silicate material from the samples (e.g., Lea et al., 2005). In this study, aluminosilicate contaminants were found in both cleaned and uncleaned *U. peregrina* specimens, and SEM/EDS analysis revealed that these contained Mg, Na, K, and other metals. However, none of the usual contaminant indicators (Al, Fe, Mn, Ti) are consistently or significantly (95% confidence level) correlated with high Mg/Ca in foraminifer tests (Fig. S7) as we would expect if aluminosilicate minerals were responsible. The pattern of elevated Mg/Ca also requires a mechanism that would cause contamination to affect some sites and not others. There is the possibility that different depositional environments or grain sizes may play a role (i.e. fine-grained particles may be harder to remove), but this still fails to address why indicators like Al/Ca do not correlate with Mg/Ca.

Finally, the LA-ICP-MS results introduce evidence against the contamination hypothesis: The average

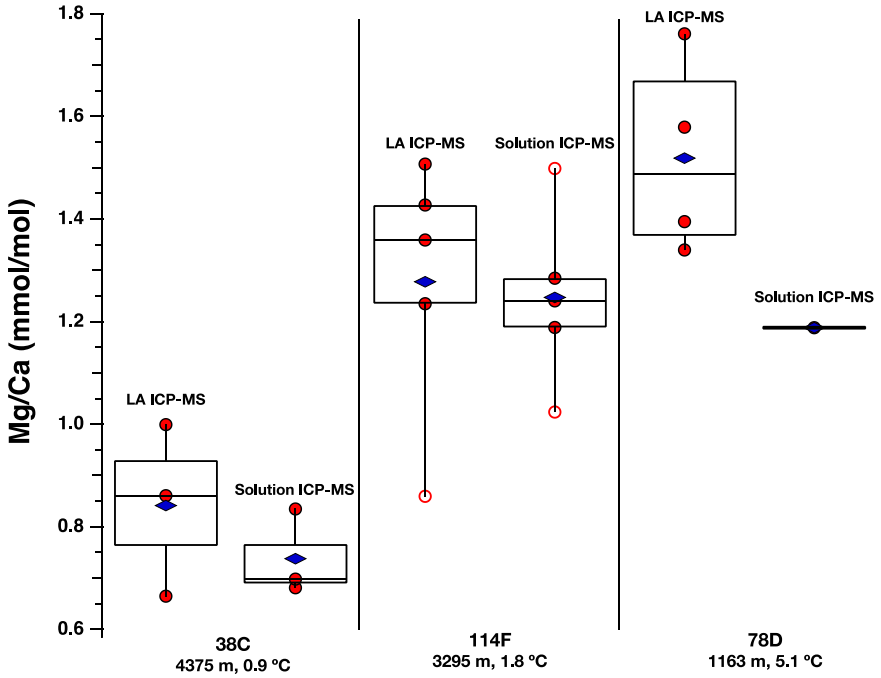

Fig. 6. Comparison of laser ablation (LA) ICP-MS results with solution methods. For LA ICP-MS, each red dot represents the average Mg/Ca of a single *U. peregrina* specimen. For solution ICP-MS, each red dot represents the average Mg/Ca of several (~10) *U. peregrina* specimens crushed and dissolved together. Blue rhombuses indicate the mean of the population.

Mg/Ca value agrees within 2SE between the two methods used in this study (Fig. 6; Table 1). The laser ablation lines were specifically drawn along the center line of chamber walls so they should not include any contaminant coatings on the inner or outer surface, where contaminants are most likely concentrated. Solution and LA-ICP-MS methods have previously been shown to achieve comparable results (e.g., Marr et al., 2013; Fehrenbacher et al., 2020). It should be noted that the LA-ICP-MS analyses in this study were performed on uncleaned specimens, while the solution ICP-MS analyses were performed on specimens cleaned using both oxidative and reductive methods. Because of this, there could be an offset between the two methods. To determine whether this alters our interpretation of the results, LA-ICP-MS Mg/Ca ratios were adjusted downward by 10 % to simulate the effect of reductive cleaning (Barker et al., 2003). With this adjustment, the agreement between the two methods remains (Fig. S17) and the conclusion remains unchanged: The similarity between LA-ICP-MS and solution methods suggests that the high-Mg signature observed is located within the biogenic calcite itself rather than in a contaminant phase, pointing to a foraminifer biomineralization mechanism.

4.3. Non-thermal Controls on Mg/Ca: Morphotype and Ontogenetic effects

Biologic effects (also called "vital effects") can influence foraminiferal calcite's Mg content and often vary among taxa, making cross-species generalizations difficult (e.g., Barrientos et al., 2018; Elderfield et al., 2006; de Nooijer et al., 2014; Evans et al., 2018; Geerken et al., 2019; Hintz et al., 2006; Wit et al., 2012). The term "vital effects" encompasses the multitude of physiological factors that affect the growth and composition of foraminiferal calcite throughout the lifespan of the organism. Generally, vital effects are poorly understood and difficult to research, particularly in deep-dwelling benthic foraminifera which are challenging to raise in culture.

Observations of bilamellar calcification show that foraminifera are capable of varying their biomineralization mechanisms: primary calcite builds new test chambers and contains a higher amount of Mg than secondary calcite, which is used to thicken older chambers (Geerken et al., 2019). This versatility suggests that foraminifera may manipulate how they calcify and influence the amount of impurities that are incorporated into the calcite. Biological control means that calcification can vary between taxa, between individuals of the same species, or even within a single individual (e.g., de Nooijer et al., 2014).

Elderfield et al. (2012) hypothesized that *Uvigerina* morphology might account for some of the variability observed, suggesting that hispid and costate morphotypes incorporated Mg differently causing different average Mg/Ca ratios. This hypothesis was put forward to explain some unusually high Mg/Ca values observed downcore. The present study analyzed three different morphotypes separately (Fig. S2; Fig. S9; Fig. S10). All three morphotypes displayed elevated Mg from 2.4-3.3 km (~2 °C), contrary to expectations based on the morphology hypothesis.

Differences in life stages could also have an influence on foraminiferal calcite composition. The influence of onto-

geny on foraminifer calcification has largely focused on planktonic species, because they migrate through the water column and thus change their ambient calcification conditions. However, there is some evidence that benthic foraminifera may experience changes in calcification throughout their lifespan that are unrelated to environmental conditions (Hintz et al., 2006).

The present study observed evidence for possible ontogenetic changes in *U. peregrina* calcification throughout its lifespan. While the small sample size precludes any strong conclusions, older, smaller chambers generally had higher Mg/Ca ratios than the larger, later chambers (Fig. S18). This trend was apparent in specimens from the two shallower sites (located at 1163 m and 3295 m) while the deeper site (4375 m) showed no evidence of this trend. It is possible that the corrosive conditions in deep water masses partially dissolved the more Mg-rich portions of the test preventing the preservation of ontogenetic variations in the sediment record (e.g. Hintz et al., 2006). It is beyond the scope of the present study to fully investigate potential ontogenetic variations given the small number of individuals studied using LA-ICP-MS. However, restricting sample selection to a certain size fraction in future studies may help reduce variability introduced by ontogenetic processes.

4.4. Environmental factors: pore water chemistry

Pore water chemistry may also play a role in affecting the Mg/Ca at these sites. *U. peregrina* are infaunal, which means they grow surrounded by pore water rather than bottom water. Conservative properties like temperature and salinity of adjacent pore and bottom waters are more likely to be the same than properties such as seawater pH or $\delta^{13}C$, which can be rapidly altered by biological or diagenetic processes within the sediments. This makes diagnosing the non-temperature influence on Mg/Ca more difficult because pore water data for calibration sites are often unavailable. Pore water properties depend on the initial bottom water chemistry, on local biological activity, sediment composition, and geologic setting (McCorkle et al., 1990; Lea et al., 2005; Nähr and Bohrmann, 1999; Koho et al., 2008). We discuss these below, starting with bottom water chemistry.

Salinity can raise Mg/Ca in some shallow benthic foraminifera (e.g., Dissard et al., 2010). Whereas sensitivity studies have not been performed with *U. peregrina*, culture experiments have assessed the sensitivity of Mg/Ca to salinity in the benthic foraminifer *Ammonia tepida* (Dissard et al., 2010; Wit et al., 2013; Geerken et al., 2018). The New Zealand core-top sites have salinities ranging from 34.5 to 34.7 psu. Over this range, salinity's influence on Mg/Ca in *Ammonia tepida* would be <0.02 mmol/mol (Dissard et al., 2010; Wit et al., 2013; Geerken et al., 2018). If *U. peregrina's* sensitivity is similar to that of other low-Mg foraminifera, and pore water salinity equals bottom water salinity, the expected magnitude of salinity influence in our core-top samples is at a level similar to the analytical uncertainty. Therefore in the deep ocean around New Zealand, the salinity gradient is not likely great enough to produce the high Mg/Ca values observed at our core-top sites.

The Mg/Ca of seawater also influences Mg incorporation in foraminiferal calcite (e.g. de Nooijer et al., 2017). The average Mg/Ca ratio of seawater changes only on long (e.g., >1 Ma) timescales and is conservative in open ocean waters. It can vary in coastal waters or in areas affected by hydrothermal activity (Lebrato et al., 2020). Hydrothermal activity primarily occurs in areas < 500 m water depth in the Bay of Plenty (Pantin and Wright, 1994); the calibration sites in our study are all located >500 m and at least 50 km offshore. It is therefore possible, but unlikely, that local factors are strongly influencing seawater Mg/Ca at our sites.

Calibration sites in the northwest Indian Ocean, Sea of Okhotsk, Cape Basin, and Bay of Plenty are all located at or near the base of continental slopes. It is possible that the sedimentation regime and/or hydrological conditions at the base of slopes are influencing the environment in which *U. peregrina* calcifies. For example, these sites may accumulate fine organic material that failed to settle further upslope (e.g. Koho et al., 2008). The observed offset of up to 1‰ between $\delta^{13}C_{Uvi}$ and overlying bottom water between 2.4 – 3.3 km depth (Fig. S5) does strongly suggest that respiration of organic material likely exerts an influence on the chemistry of pore waters in the Bay of Plenty. It is also possible that methane- or CO_2-rich fluids migrating upward from below the seafloor could affect local pore waters. Subducted limestones have been hypothesized to be responsible for gas and fluid release resulting in pockmarks on Chatham Rise (Stott et al., 2019). Therefore, although we note that unexpectedly high *Uvigerina* Mg/Ca at our mid-depth sites as well as others in the northwest Indian Ocean, the Sea of Okhotsk, and the Cape Basin (Lear et al., 2002; Elderfield et al., 2006; Gussone et al., 2016) are all similarly bathed by carbon-rich, oxygen-poor deep water masses, we refrain from quantitative analysis of these parameters based on available bottom water data since $\delta^{13}C$ data as well as dissolution of planktic tests (Fig. S11) suggest the existence of pore-bottom water offsets for parameters like DIC, alkalinity, and/or oxygen.

Based on the available data, it seems unlikely that salinity or seawater Mg/Ca can account for the unexpectedly high values observed between 2.4 – 3.3 km water depth. In the absence of culture studies on *Uvigerina* species or data on pore water chemistry at calibration sites, it is difficult to conclude how additional environmental conditions such as DIC or alkalinity may be affecting Mg incorporation during calcification.

5. CONCLUSIONS

The Mg/Ca-temperature relationship in *U. peregrina* derived from surface sediments of the southwest Pacific is consistent with previously published results from other ocean regions. Application of previous calibration equations reproduces modern temperatures within ± 2 °C for sites located between 1 km and 2 km water depth. This result suggests that *U. peregrina* Mg/Ca can be useful for reconstructing intermediate water paleotemperatures in this

location, particularly at shallower sites which are more likely to experience temperature changes > 2 °C. In addition, our results indicate that the New Zealand samples act as part of a global population, allowing the application of global calibration equations to sites in this area.

Observations from 2.4 − 3.3 km depth cannot be fully explained by temperature, and we suggest that future core-top studies with *Uvigerina* must also include data on pore-water chemistry ([Mg], [Ca], oxygen, and carbonate system parameters). Further research into the biomineralization of *U. peregrina* under different pore water conditions could clarify whether a non-temperature influence is affecting Mg incorporation at deep sites. It is important to resolve this issue; the occurrence of anomalously high Mg/Ca at low temperatures (<2 °C) in *Uvigerina* skews the global core-top regression and could help explain why a modern core-top regression (ΔMg/Ca (mmol/mol) / ΔT(°C) = 0.07) yielded unreasonable glacial bottom water temperatures compared to a $\delta^{18}O_{sw}$-constrained estimate corresponding to a higher sensitivity (ΔMg/Ca (mmol/mol) / ΔT(°C) = 0.1) (Elderfield et al., 2010).

Until the non-temperature control on *U. peregrina* observed here can be better diagnosed, we recommend screening core sites to assess whether the *Uvigerina* Mg/Ca-temperature proxy is suitable for that site. Core-top Mg/Ca should be used to determine whether measured and predicted temperatures agree. Where possible, analyzing specimens from a restricted size range or combining *Uvigerina* measurements with those of epifaunal species or other infaunal species could also help assess variable pore water influences. If the high-Mg signature is biological in origin, it is likely that different taxa will exhibit different responses. The verification of *Uvigerina*-based paleotemperature records with other, independent proxies is recommended to confirm whether *Uvigerina* Mg/Ca remains a reliable indicator of temperature through time.

Declaration of Competing Interest

The authors declare that there is no conflict of interest.

ACKNOWLEDGMENTS

Funding for this project was provided by NSF OCE 1634423, awarded to KA and ES. We gratefully acknowledge the assistance of Benjamin Lindsay, Jonathan Maurer, Ryan Bu, Martin Yates, and Brenda Hall. Many thanks to three anonymous reviewers who provided detailed and constructive feedback on this work.

APPENDIX A. SUPPLEMENTARY MATERIAL

Supplementary data to this article can be found online at https://doi.org/10.1016/j.gca.2021.06.015.

REFERENCES

Allen K. A., Sikes E. L., Hönisch B., Elmore A. C., Guilderson T. P., Rosenthal Y. and Anderson R. F. (2015) Southwest Pacific deep water carbonate chemistry linked to high southern latitude climate and atmospheric CO2 during the Last Glacial Termination. *Quat. Sci. Rev.* **122**, 180–191.

Anand P., Elderfield H. and Conte M. H. (2003) Calibration of Mg/Ca thermometry in planktonic foraminifera from a sediment trap time series. *Paleoceanography* **18**, n/a-n/a.

Barker S., Greaves M. and Elderfield H. (2003) A study of cleaning procedures used for foraminiferal Mg/Ca paleothermometry. *Geochem. Geophys. Geosyst.* **4**, n/a-n/a.

Barrientos N., Lear C. H., Jakobsson M., Stranne C., O'Regan M., Cronin T. M., Gukov A. Y. and Coxall H. K. (2018) Arctic Ocean benthic foraminifera Mg/Ca ratios and global Mg/Ca-temperature calibrations: new constraints at low temperatures. *Geochim. Cosmochim. Acta*.

Berger W. H. (1970) Planktonic Foraminifera: Selective solution and the lysocline. *Mar Geol* **8**, 111–138.

Boyle E. A. and Keigwin L. D. (1985) Comparison of Atlantic and Pacific paleochemical records for the last 215,000 years: changes in deep ocean circulation and chemical inventories. *Earth Planet. Sci. Lett.* **76**, 135–150.

Branson O., Read E., Redfern S. A., Rau C. and Elderfield H. (2015) Revisiting diagenesis on the Ontong Java Plateau: Evidence for authigenic crust precipitation inGloborotalia tumida: Foram Dissolution and Reprecipitation. *Paleoceanography* **30**.

Brown S. J. and Elderfield H. (1996) Variations in Mg/Ca and Sr/Ca ratios of planktonic foraminifera caused by postdepositional dissolution: Evidence of shallow Mg-dependent dissolution. *Paleoceanography* **11**, 543–551.

Bryan S. P. and Marchitto T. M. (2008) Mg/Ca–temperature proxy in benthic foraminifera: New calibrations from the Florida Straits and a hypothesis regarding Mg/Li. *Paleoceanography* **23**, n/a-n/a.

Chanda P., Gorski C. A., Oakes R. L. and Fantle M. S. (2019) Low temperature stable mineral recrystallization of foraminiferal tests and implications for the fidelity of geochemical proxies. *Earth Planet. Sci. Lett.* **506**, 428–440.

Chave K., Deffeyes K., Weyl P. and … G.-R. (1962) Observations on the solubility of skeletal carbonates in aqueous solutions.

Cléroux C., Cortijo E., Duplessy J.-C. and Zahn R. (2007) Deep-dwelling foraminifera as thermocline temperature recorders: Temperature from Foraminifera. *Geochem Geophys Geosystems* **8**, n/a-n/a.

Dickson A., Sabine C. L. and Christian J. (2007) Guide to best practices for ocean CO2 measurements. *North Pacific Marine Science*, Organization.

Dissard D., Nehrke G., Reichart G. and Bijma J. (2010) The impact of salinity on the Mg/Ca and Sr/Ca ratio in the benthic foraminifera Ammonia tepida: Results from culture experiments. *Geochim. Cosmochim. Acta* **74**, 928–940.

Elderfield H., Yu J., Anand P., Kiefer T. and Nyland B. (2006) Calibrations for benthic foraminiferal Mg/Ca paleothermometry and the carbonate ion hypothesis. 250.

Elderfield H., Greaves M., Barker S., Hall I. R., Tripati A., Ferretti P., Crowhurst S., Booth L. and Daunt C. (2010) A record of bottom water temperature and seawater δ18O for the Southern Ocean over the past 440kyr based on Mg/Ca of benthic foraminiferal Uvigerina spp. *Quat. Sci. Rev.* **29**, 160–169.

Elderfield H., Ferretti P., Greaves M., Crowhurst S., McCave I., Hodell D. and Piotrowski A. (2012) Evolution of Ocean Temperature and Ice Volume Through the Mid-Pleistocene Climate Transition. Science 337.

Evans D., Müller W. and Erez J. (2018) Assessing foraminifera biomineralisation models through trace element data of cultures under variable seawater chemistry. *Geochim. Cosmochim. Acta*.

Fehrenbacher J., Marchitto T. and Spero H. J. (2020) Comparison of Laser Ablation and Solution-Based ICP-MS Results for

Individual Foraminifer Mg/Ca and Sr/Ca Analyses. *Geochem Geophys Geosystems* **21**.

Geerken E., Nooijer L. de, Dijk I. van and Reichart G.-J. (2018) Impact of salinity on element incorporation in two benthic foraminiferal species with contrasting magnesium contents. Biogeosciences 15, 2205–2218.

Geerken E., Nooijer L. de, Roepert A., Polerecky L., King H. and Reichart G. (2019) Element banding and organic linings within chamber walls of two benthic foraminifera. Scientific Reports 9, 3598.

Groeneveld J. and Chiessi C. M. (2011) Mg/Ca of Globorotalia inflata as a recorder of permanent thermocline temperatures in the South Atlantic. *Paleoceanography* **26**, n/a-n/a.

Gussone N., Filipsson H. L. and Kuhnert H. (2016) Mg/Ca, Sr/Ca and Ca isotope ratios in benthonic foraminifers related to test structure, mineralogy and environmental controls. *Geochim. Cosmochim. Acta* **173**, 142–159.

Hintz C. J., Shaw T. J., Bernhard J. M., Chandler T. G., McCorkle D. C. and Blanks J. K. (2006) Trace/minor element:calcium ratios in cultured benthic foraminifera. Part II: Ontogenetic variation. *Geochim. Cosmochim. Acta* **70**, 1964–1976.

Johnstone H., Lee W. and Schulz M. (2016) Effect of preservation state of planktonic foraminifera tests on the decrease in Mg/Ca due to reductive cleaning and on sample loss during cleaning. *Chem. Geol.* **420**, 23–36.

Jorissen F. J., Stigter H. C. de and Widmark J. (1995) A conceptual model explaining benthic foraminiferal microhabitats. Marine Micropaleontology 26, 3–15.

Koho K. A., García R., de Stigter H. C., Epping E. and Koning E. (2008) Sedimentary labile organic carbon and pore water redox control on species distribution of benthic foraminifera: A case study from Lisbon-Setúbal Canyon (southern Portugal). *Prog. Ocean.* **79**, 55–82.

Lea D. W., Pak D. K. and Paradis G. (2005) Influence of volcanic shards on foraminiferal Mg/Ca in a core from the Galápagos region. *Geochem. Geophys. Geosyst.* **6**, n/a-n/a.

Lear C. H., Rosenthal Y. and Slowey N. (2002) Benthic foraminiferal Mg/Ca-paleothermometry: a revised core-top calibration. *Geochim. Cosmochim. Acta* **66**, 3375–3387.

Lebrato M., Garbe-Schönberg D., Müller M. N., Blanco-Ameijeiras S., Feely R. A., Lorenzoni L., Molinero J.-C., Bremer K., Jones D. O. B., Iglesias-Rodriguez D., Greeley D., Lamare M. D., Paulmier A., Graco M., Cartes J., Ramos J. B. e, Lara A. de, Sanchez-Leal R., Jimenez P., Paparazzo F. E., Hartman S. E., Westernströer U., Küter M., Benavides R., Silva A. F. da, Bell S., Payne C., Olafsdottir S., Robinson K., Jantunen L. M., Korablev A., Webster R. J., Jones E. M., Gilg O., Bois P. B. du, Beldowski J., Ashjian C., Yahia N. D., Twining B., Chen X.-G., Tseng L.-C., Hwang J.-S., Dahms H.-U. and Oschlies A. (2020) Global variability in seawater Mg:Ca and Sr:Ca ratios in the modern ocean. Proc National Acad Sci 117, 22281–22292.

Lowe D. J., Blaauw M., Hogg A. G. and Newnham R. M. (2013) Ages of 24 widespread tephras erupted since 30,000 years ago in New Zealand, with re-evaluation of the timing and palaeoclimatic implications of the Lateglacial cool episode recorded at Kaipo bog. *Quaternary Sci Rev* **74**, 170–194.

Marchitto T. M., Curry W. B., Lynch-Stieglitz J., Bryan S. P., Cobb K. M. and Lund D. C. (2014) Improved oxygen isotope temperature calibrations for cosmopolitan benthic foraminifera. 130.

Marr J. P., Bostock H. C., Carter L., Bolton A. and Smith E. (2013) Differential effects of cleaning procedures on the trace element chemistry of planktonic foraminifera. *Chem. Geol.* **351**, 310–323.

McCave I., Carter L. and Hall I. (2008) Glacial-interglacial changes in water mass structure and flow in the SW Pacific Ocean. 27.

McCorkle D. C., Keigwin L. D., Corliss B. H. and Emerson S. R. (1990) The influence of microhabitats on the carbon isotopic composition of deep-sea benthic foraminifera. *Paleoceanography*, 5.

Nähr T. H. and Bohrmann G. (1999) Barium-rich authigenic clinoptilolite in sediments from the Japan Sea—a sink for dissolved barium?. *Chem. Geol.* **158**, 227–244.

de Nooijer L. J., Spero H. J., Erez J., Bijma J. and Reichart G. J. (2014) Biomineralization in perforate foraminifera. *Earth Sci. Rev.* **135**, 48–58.

de Nooijer L., van Dijk I., Toyofuku T. and Reichart G. (2017) The Impacts of Seawater Mg/Ca and Temperature on Element Incorporation in Benthic Foraminiferal Calcite. *Geochem. Geophys. Geosyst.* **18**, 3617–3630.

Olsen A., Lange N., Key R. M., Tanhua T., Álvarez M., Becker S., Bittig H. C., Carter B. R., Cunha L. da, Feely R. A., Heuven S. van, Hoppema M., Ishii M., Jeansson E., Jones S. D., Jutterström S., Karlsen M. K., Kozyr A., Lauvset S. K., Monaco C., Murata A., Pérez F. F., Pfeil B., Schirnick C., Steinfeldt R., Suzuki T., Telszewski M., Tilbrook B., Velo A. and Wanninkhof R. (2019) GLODAPv2.2019 – an update of GLODAPv2. Earth System Science Data Discussions, 1–39.

Oomori T., Kaneshima H., Maezato Y. and Kitano Y. (1987) Distribution coefficient of Mg2+ ions between calcite and solution at 10–50°C. *Mar. Chem.* **20**, 327–336.

Pantin H. M. and Wright I. C. (1994) Submarine hydrothermal activity within the offshore Taupo Volcanic Zone, Bay of Plenty continental shelf, New Zealand. *Cont Shelf Res* **14**, 1411–1438.

Raymo M. E., Kozdon R., Evans D., Lisiecki L. and Ford H. L. (2018) The accuracy of mid-Pliocene δ18O-based ice volume and sea level reconstructions. *Earth Sci. Rev.* **177**.

Regenberg M., Regenberg A., Garbe-Schönberg D. and Lea D. W. (2014) Global dissolution effects on planktonic foraminiferal Mg/Ca ratios controlled by the calcite-saturation state of bottom waters. *Paleoceanography* **29**, 127–142.

Rosenthal Y., Boyle E. A. and Slowey N. (1997a) Temperature control on the incorporation of magnesium, strontium, fluorine, and cadmium into benthic foraminiferal shells from Little Bahama Bank: Prospects for thermocline paleoceanography. *Geochim. Cosmochim. Acta* **61**, 3633–3643.

Rosenthal Y., Boyle E. A. and Labeyrie L. (1997b) Last glacial maximum paleochemistry and deepwater circulation in the Southern Ocean: Evidence from foraminiferal cadmium. *Paleoceanography* **12**.

Rosenthal Y., Field M. and Sherrell R. (1999) Precise determination of element/calcium ratios in calcareous samples using sector field inductively coupled plasma mass spectrometry. *Anal. Chem.* **71**, 3248–3253.

Ryan W. B. F., Carbotte S. M., Coplan J. O., O'Hara S., Melkonian A., Arko R., Weissel R. A., Ferrini V., Goodwillie A., Nitsche F., Bonczkowski J. and Zemsky R. (2009) Global Multi-Resolution Topography synthesis. *Geochem Geophys Geosystems* **10**, n/a-n/a.

Sadekov A., Eggins S. M., Klinkhammer G. P. and Rosenthal Y. (2010) Effects of seafloor and laboratory dissolution on the Mg/Ca composition of Globigerinoides sacculifer and Orbulina universa tests — A laser ablation ICPMS microanalysis perspective. *Earth Planet. Sci. Lett.* **292**, 312–324.

Schlitzer R. (2018) Ocean Data View.

Schmidt G. A., Bigg G. R. and Rohling E. J. (1999) Global Seawater Oxygen-18 Database - v1.22.

Schweizer M., Pawlowski J., Duijnstee I. A. P., Kouwenhoven T. J. and van der Zwaan G. J. (2005) Molecular phylogeny of the foraminiferal genus Uvigerina based on ribosomal DNA sequences. *Mar. Micropaleontol.* **57**.

Shackleton N. J. (1987) Oxygen isotopes, ice volume and sea level. *Quaternary Sci Rev* **6**, 183–190.

Shane P., Sikes E. L. and Guilderson T. P. (2006) Tephra beds in deep-sea cores off northern New Zealand: implications for the history of Taupo Volcanic Zone, Mayor Island and White Island volcanoes. *J. Volcan. Geo. Res.* **154**, 276–290.

Sikes E. L., Cook M. S. and Guilderson T. P. (2016a) Reduced deep ocean ventilation in the Southern Pacific Ocean during the last glaciation persisted into the deglaciation. *Earth Planet. Sci. Lett.* **438**, 130–138.

Sikes E. L., Elmore A. C., Allen K. A., Cook M. S. and Guilderson T. P. (2016) Glacial water mass structure and rapid δ18O and δ13C changes during the last glacial termination in the Southwest Pacific. 456.

Sikes E. L., Allen K. A. and Lund D. C. (2017) Enhanced δ13C and δ18O Differences Between the South Atlantic and South Pacific During the Last Glaciation: The Deep Gateway Hypothesis. *Paleoceanography* **32**, 1000–1017.

Skinner L., McCave I. N., Carter L., Fallon S., Scrivner A. E. and Primeau F. (2014) Reduced ventilation and enhanced magnitude of the deep Pacific carbon pool during the last glacial period. *Earth Planet. Sci. Lett.* **411**, 45–52.

Stott L., Davy B., Shao J., Coffin R., Pecher I., Neil H., Rose P. and Bialas J. (2019) CO 2 Release From Pockmarks on the Chatham Rise-Bounty Trough at the Glacial Termination. *Paleoceanogr Paleoclimatology* **34**, 1726–1743.

Talley L. (2013) Closure of the Global Overturning Circulation Through the Indian, Pacific, and Southern Oceans: Schematics and Transports. *Oceanography* **26**, 80–97.

Tukey J. W. (1977) *Exploratory Data Analysis*. Wesley Publishing Company.

Waelbroeck C., Labeyrie L., Michel E., Duplessy J. C., McManus J. F., Lambeck K., Balbon E. and Labracherie M. (2002) Sea-level and deep water temperature changes derived from benthic foraminifera isotopic records. *Quat. Sci. Rev.* **21**, 295–305.

Weldeab S., Arce A. and Kasten S. (2016) Mg/Ca- Δ CO 3 pore water 2 − –temperature calibration for Globobulimina spp.: A sensitive paleothermometer for deep-sea temperature reconstruction. *Earth Planet Sc Lett* **438**, 95–102.

Williams D. F., Ehrlich R., Spero H. J., Healy-Williams N. and Gary A. C. (1988) Shape and isotopic differences between conspecific foraminiferal morphotypes and resolution of paleoceanographic events. *Palaeogeogr Palaeoclim Palaeoecol* **64**, 153–162.

Wit J., Nooijer L. de, Barras C., Jorissen F. and Reichart G. (2012) A reappraisal of the vital effect in cultured benthic foraminifer Bulimina marginata on Mg/Ca values: assessing temperature uncertainty relationships. Biogeosciences 9, 3693–3704.

Wit J., Nooijer L. de, Wolthers M. and Reichart G. (2013) A novel salinity proxy based on Na incorporation into foraminiferal calcite. Biogeosciences 10, 6375–6387.

Yu J. and Elderfield H. (2008) Mg/Ca in the benthic foraminifera Cibicidoides wuellerstorfi and Cibicidoides mundulus: Temperature versus carbonate ion saturation. *Earth Planet. Sci. Lett.* **276**, 129–139.

Associate editor: Thomas M. Marchitto